Infrared Spectra, Structure, and Bonding of the Group 6 and Ammonia M:NH_3, H_2N-MH, and $N\equiv MH_3$ Reaction Products in Solid Argon

Xuefeng Wang and Lester Andrews*

Department of Chemistry, University of Virginia, Charlottesville, Virginia 22904-4319

Received April 17, 2008

Laser-ablated chromium, molybdenum, and tungsten atoms undergo oxidative addition reactions with ammonia during condensation in excess argon. The subject molecules were trapped in solid argon and identified by isotopic shifts and DFT frequency calculations. The 1:1 metal−ammonia complexes increased on annealing and photoisomerized to H_2N-MH and then to $N\equiv MoH_3$ and $N\equiv WH_3$, but $N\equiv CrH_3$ is too high in energy to be formed here. These products also increased slightly on annealing, which indicates a spontaneous reaction between group 6 metal atoms and ammonia. The $N\equiv MoH_3$ and $N\equiv WH_3$ molecules contain fully developed triple bonds with effective bond orders of 2.91 and 2.92, computed using the B3LYP density functional, and terminal metal nitride bond lengths, in agreement with those measured for larger organometallic complexes.

Introduction

Investigations of the oxidative addition of the N−H bond of ammonia or amines to transition-metal centers are important for understanding life sciences, catalytic processes, and nitrogen fixation.[1−3] Examples of the resulting transition-metal organometallic complexes have received considerable attention, including theoretical computations of the simple nitrido Mo and W trihydrides.[4−10] Previous investigations of the reaction of thermally produced late-transition-metal atoms (Fe, Ni, Cu) with NH_3 formed the 1:1 complex (M:NH_3) adducts, which rearrange to H_2N-MH under ultraviolet irradiation.[11−13] Recently laser-ablated early transition metal atom (Sc, Ti, V, Zr, Hf) reactions with NH_3 gave analogous H_2N-MH products, which rearranged further to $HN=MH_2$.[14] The most recent study shows that the thorium atom reaction with NH_3 is very dramatic: on deposition and annealing a high yield of $HN=ThH_2$ is formed, suggesting that f orbitals are strongly involved in the bonding.[15]

The chemistry of group 6 metals (Cr, Mo, W) reveals interesting family trends. Since different d orbitals participate in bonding, the tungsten and molybdenum compounds favor high oxidation states, while the chromium counterparts are stabilized in low oxidation states. For example, group 6 metal atoms react with H_2O_2, giving high-oxidation-state H_2WO_2 and H_2MoO_2 and low-oxidation-state $Cr(OH)_2$, respectively.[16] Tungsten and molybdenum atoms react with H_2 in solid neon to give trigonal-prismatic C_{3v} hexahydrides, WH_6 and MoH_6, while only the hydride complex $CrH_2(H_2)_2$ is obtained for chromium.[17] Further explorations of group 6 metal reactions with other specific molecules will enrich our knowledge of chemical bonding models.

We present here a matrix infrared spectroscopic investigation of laser-ablated Cr, Mo, and W atom reactions with NH_3 in solid argon. The most interesting new products, the $N\equiv MoH_3$ and $N\equiv WH_3$ complexes, are simple models of larger organometallic nitride complexes[18,19] and are isoelectronic with the methane reaction product methylidyne molecules $HC\equiv MoH_3$,

* To whom correspondence should be addressed. E-mail: lsa@virginia.edu.

(1) (a) Hille, R. *Chem. Rev.* **1996**, *96*, 2757. (b) Johnson, M. K.; Rees, D. C.; Adams, W. W. *Chem. Rev.* **1996**, *96*, 2817.

(2) Tsang, J. Y. K.; Fujita-Takayama, C.; Buschhaus, M. S. A.; Patrick, B. O.; Legzdins, P. *J. Am. Chem. Soc.* **2006**, *128*, 14762.

(3) Cotton, F. A.; Wilkinson, G.; Murillo, C. A.; Bochmann, M. *Advanced Inorganic Chemistry*, 6th ed.; Wiley: New York, 1999.

(4) Macgregor, S. A. *Organometallics* **2001**, *20*, 1860.

(5) Zhao, J.; Goldman, A. S.; Hartwig, J. F. *Science* **2005**, *307*, 1080, and references therein.

(6) Xue, W. N.; Chen, M. C. W.; Mak, T. C. W.; Che, C. M. *Inorg. Chem.* **1997**, *36*, 6437.

(7) Fang, G. S.; Huang, J. S.; Zhu, N. Y.; Che, C. M. *Eur. J. Inorg. Chem.* **2004**, 1341.

(8) Berry, J. F.; Bill, E.; Bothe, E.; George, S. D.; Mienert, B.; Neese, F.; Wieghardt, K. *Science* **2006**, *312*, 1937.

(9) Petrenko, T.; George, S. D.; Aliaga-Alcalde, N.; Bill, E.; Mienert, B.; Xiao, Y.; Guo, Y.; Sturhahn, W.; Cramer, S. P.; Wieghardt, K.; Neese, F. *J. Am. Chem. Soc.* **2007**, *129*, 11053, and references therein.

(10) Firman, T. K.; Landis, C. R. *J. Am. Chem. Soc.* **2001**, *123*, 11728, and references therein.

(11) Hauffman, J. W.; Hauge, R. H.; Margrave, J. L. *High Temp. Sci.* **1984**, *17*, 237.

(12) (a) Ball, D. W.; Hauge, R. H.; Margrave, J. L. *High Temp. Sci.* **1988**, *25*, 95. (b) Ball, D. W.; Hauge, R. H.; Margrave, J. L. *Inorg. Chem.* **1989**, *28*, 1599.

(13) Szczepanski, J.; Szczesniak, M.; Vala, M. *Chem. Phys. Lett.* **1989**, *162*, 123.

(14) (a) Zhou, M.; Chen, M.; Zhang, L.; Lu, H. *J. Phys. Chem. A* **2002**, *106*, 11456 (Sc, Ti, V + NH_3). (b) Zhou, M.; Chen, M.; Zhang, L.; Lu, H. *J. Phys. Chem. A* **2002**, *106*, 9017 (Zr, Hf + NH_3).

(15) Wang, X.; Andrews, L.; Marsden, C. J. *Chem. Eur. J.* **2007**, *13*, 5601 (Th + NH_3).

(16) Wang, X.; Andrews, L. *J. Phys. Chem. A* **2006**, *110*, 10409 (group 6 + H_2O_2).

(17) (a) Wang, X.; Andrews, L. *J. Am. Chem. Soc.* **2002**, *124*, 5636 (WH_6). (b) Wang, X.; Andrews, L. *J. Phys. Chem. A* **2003**, *107*, 570 (Cr + H_2). (c) Wang, X.; Andrews, L. *J. Phys. Chem. A* **2005**, 9021 (Mo + H_2).

(18) Gebeyehu, Z.; Weller, B.; Neumuller, K.; Dehnicke, K. *Z. Anorg. Allg. Chem.* **1991**, *593*, 99 (R_3MoN bond lengths)See also: Geyer, A. M.; Gdula, R. L.; Wiedner, E. S.; Johnson, M. J. A. *J. Am. Chem. Soc.* **2007**, *129*, 3900.

(19) Clough, C. R.; Greco, J. B.; Figueroa, J. S.; Diaconescu, P. L.; Davis, W. M.; Cummins, C. C. *J. Am. Chem. Soc.* **2004**, *126*, 7742 (R_3WN bond lengths). See also: Fox, A. R.; Clough, C. R.; Piro, N. A.; Cummins, C. C. *Angew. Chem., Int. Ed.* **2007**, *46*, 973.

10.1021/om8003459 CCC: $40.75
Publication on Web 09/10/2008

and $HC{\equiv}WH_3$ prepared earlier in this laboratory.[20] These new species have been identified from matrix isolation infrared spectroscopy, comparison to the results of similar investigations with NF_3,[21] and theoretical vibrational frequency calculations.

Experimental and Computational Methods

The experiments for laser-ablated Cr, Mo, and W atom reactions and for ammonia in excess argon at 8 K have been described in our previous papers.[16,17,20−22] Because of wall adsorption, ammonia concentrations in the matrix are only approximate, but we estimate the concentrations used here to be near 0.3% ammonia in argon. The Nd:YAG laser fundamental (1064 nm, 10 Hz repetition rate with 10 ns pulse width) was focused onto the rotating metal target (Johnson Matthey), which gave a bright plume spreading uniformly to the cold CsI window. The metal targets were polished to remove oxide coating and immediately placed in the vacuum chamber. The laser energy was varied about 10−20 mJ/pulse. FTIR spectra were recorded at 0.5 cm^{-1} resolution on a Nicolet 750 instrument with 0.1 cm^{-1} measurement accuracy using an MCTB detector. Isotopic samples ($^{15}NH_3$, ND_3) were used as received, and ND_3 was codeposited directly from the cylinder through a leak valve to avoid isotopic contamination (we estimate >90% D survival). Matrix samples were annealed at different temperatures, and selected samples were subjected to photolysis by a medium-pressure mercury arc lamp (Philips, 175 W) with the globe removed.

Following our successful use of density functional theory to calculate structures and frequencies for analogous group 6 metal atom reaction products with methane,[20] complementary DFT calculations were performed for the ammonia system using the Gaussian 03 program,[23] the B3LYP and BPW91 functionals, the 6-311+G(3df,3pd) basis set for hydrogen and nitrogen atoms, and the SDD pseudopotential for metal atoms.[24−27] All of the geometrical parameters were fully optimized, and the optimized geometry was confirmed by vibrational analysis. Harmonic vibrational frequencies were calculated analytically with zero-point energy included for the determination of reaction energies. Natural bond orbital (NBO)[23,28] analysis was also done to explore the bonding in new metal nitrido trihydride product molecules.

Results

Infrared spectra of products formed in the reactions of laser-ablated chromium, molybdenum, and tungsten atoms with NH_3 in excess argon during condensation at 8 K will be presented in turn. Density functional calculations were performed to support the identifications of new reaction products. Common species, such as NH_2, Ar_nH^+, and metal oxides have been identified in previous papers.[29−31]

Table 1. Infrared Absorptions (cm^{-1}) Observed for Products of the Reaction of W, Mo, and Cr Atoms and NH_3, $^{15}NH_3$, and ND_3 Isotopic Molecules

NH_3	$^{15}NH_3$	ND_3	assignt
		W	
1924.1	1924.1	1377.0	NWH_3 (a_1, W−H str)
1917.0	1917.0	1377.0	NWH_3 (e, W−H str)
1911.1	1911.1	1375.0	NWH_3 (W−H str) (site)
1772.2	1772.2	1272.3	H_2NWH (W−H str)
1770.9	1770.9	1271.6	H_2NWH (W−H str) (site)
1188.0	1181.8	covered[a]	W:NH_3 (1:1 complex)
1092.2	1058.4	covered	NWH_3 (W−N str)
		Mo	
1815.4	1815.4	covered	$NMoH_3$ (e,Mo−H str)
1761			NMoH
1704.5	1704.5	1232.7	H_2NMoH (Mo−H str)
1081	covered	covered	NWH_3 (Mo−N str)
1100.8	1094.9	covered	Mo:NH_3 (1:1 complex)
1097.6	1091.7	covered	Mo:NH_3 (1:1 complex)
		Cr	
1614.3	1614.3	1165.0	H_2NCrH (Cr−H str)
1100.2	1095.8	covered	Cr:NH_3 (1:1 complex)
1095.0	1090.4	covered	Cr:NH_3 (1:1 complex)

[a] Unfortunately, owing to the complication of ammonia aggregates and isotopic H/D exchange, many regions where new bands are expected are covered. The methane impurity band (from cracking silicone diffusion pump oil) covers the expected $NMoD_3$ absorption.

Tungsten. Laser-ablated W atoms were codeposited with NH_3 in argon; the product absorptions are given in Table 1, and representative spectra are shown in Figure 1. Many experiments were performed using different substrate temperatures, laser energies, and ammonia concentrations in order to optimize product yields and minimize complications from ammonia clusters. In the W−H stretching region bands at 1924.1 and 1917.0 cm^{-1} were observed after deposition, and they increased slightly on 20 K annealing, increased on >470 nm irradiation, but decreased on 240−380 nm irradiation. A new weak band at 1092.2 cm^{-1} tracks with the upper bands on annealing and irradiation. A site-split doublet at 1772.2, 1770.9 cm^{-1} decreases on annealing, disappears on >470 nm irradiation, but is restored with 240−380 nm light. A very weak band at 1188.0 cm^{-1} increases markedly on first annealing, disappears on >470 nm irradiation, but returns on further annealing. It appears that these product species are converted into each other on photochemical rearrangement.

Isotopic labeling experiments were done using $^{15}NH_3$ and ND_3 samples (Figures 1 and 2). The W−H stretching frequencies with $^{15}NH_3$ were essentially the same as those with NH_3, but the weak band at 1092.2 cm^{-1} shifted to 1058.4 cm^{-1} in the ammonia cluster region: these bands increased together on >470 nm irradiation. With ND_3 the upper bands shifted into the W−D stretching region at 1377.0 and 1272.3, 1271.6 cm^{-1}.

Molybdenum. Infrared spectra of laser-ablated molybdenum atom reaction products with NH_3 in argon are shown in Figure 3, and the absorptions are also given in Table 1. In the Mo−H stretching region a sharp band at 1815.4 cm^{-1} appeared on deposition, increased on annealing, increased markedly on >320 nm irradiation, but decreased on 240−380 nm irradiation. Weak

(20) (a) Andrews, L.; Cho, H.-G. *Organometallics* **2006**, *25*, 4040 (review article). (b) Cho, H.-G.; Andrews, L. *J. Am. Chem. Soc.* **2005**, *127*, 8226 (Mo + CH_4). (c) Cho, H.-G.; Andrews, L.; Marsden, C. *Inorg. Chem.* **2005**, *44*, 7634 (W + CH_4).

(21) Wang, X.; Andrews, L.; Lindh, R.; Veryazov, V.; Roos, B. O. *J. Phys. Chem. A* **2008**, *112*, 8030 (group 6 metals + NF_3, PF_3).

(22) (a) Andrews, L. *Chem. Soc. Rev.* **2004**, *33*, 123. (b) Andrews, L.; Citra, A. *Chem. Rev.* **2002**, *102*, 885.

(23) Kudin, K. N., et al. Gaussian 03, Revision D.01, Gaussian, Inc., Pittsburgh, PA, 2004.

(24) (a) Becke, A. D. *J. Chem. Phys.* **1993**, *98*, 5648. (b) Lee, C.; Yang, Y.; Parr, R. G. *Phys. Rev. B* **1988**, *37*, 785.

(25) Perdew, J. P.; Burke, K.; Wang, Y. *Phys. Rev. B* **1996**, *54*, 16533, and references therein.

(26) Frisch, M. J.; Pople, J. A.; Binkley, J. S. *J. Chem. Phys.* **1984**, *80*, 3265.

(27) Andrae, D.; Haeussermann, U.; Dolg, M.; Stoll, H.; Preuss, H. *Theor. Chim. Acta* **1990**, *77*, 123.

(28) (a) Reed, A. E.; Weinstock, R. B.; Weinhold, F. *J. Chem. Phys.* **1985**, *83*, 735. (b) Reed, A. E.; Curtiss, R. B.; Weinhold, F. *Chem. Rev.* **1988**, *88*, 899.

(29) Milligan, D. E.; Jacox, M. E. *J. Chem. Phys.* **1965**, *43*, 4487 (NH_2).

(30) (a) Wight, C. A.; Ault, B. S.; Andrews, L. *J. Chem. Phys.* **1976**, *65*, 1244. (b) Milligan, D. E.; Jacox, M. E. *J. Mol. Spectrosc.* **1973**, *46*, 460 (Ar_nH^+).

(31) Bare, W. D.; Souter, P. F.; Andrews, L. *J. Phys. Chem. A* **1998**, *102*, 8279 (metal oxides with resolved Mo isotopic splittings).

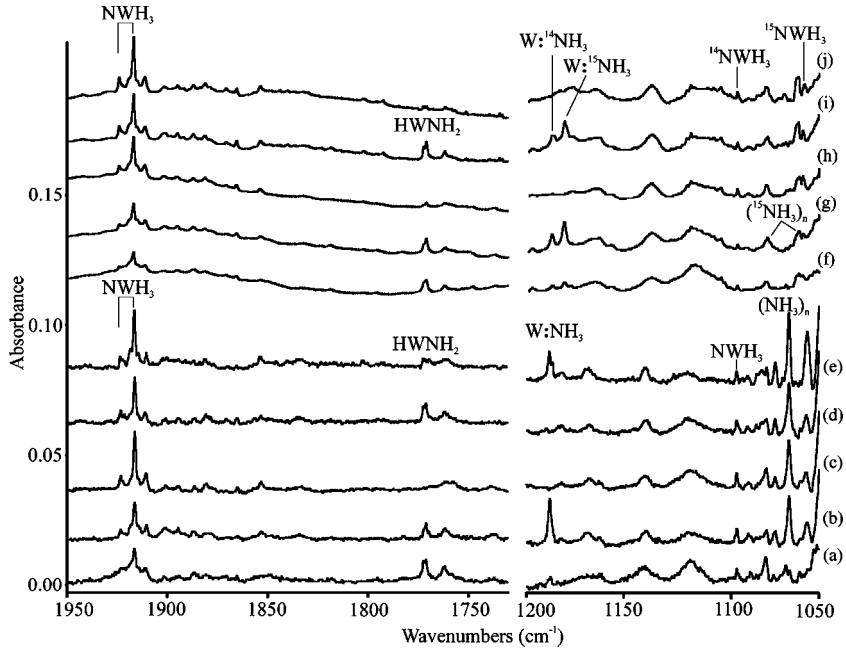

Figure 1. Infrared spectra for the tungsten atom and NH_3 reaction products in solid argon at 8 K: (a) W + NH_3 deposition for 60 min; (b) after annealing to 20 K; (c) after >470 nm irradiation; (d) after 240−380 nm irradiation; (e) after annealing to 30 K; (f) W + $^{15}NH_3$ (75% survival) deposition for 60 min; (g) after annealing to 20 K; (h) after >470 nm irradiation; (i) after annealing to 25 K; (j) after another >470 nm irradiation.

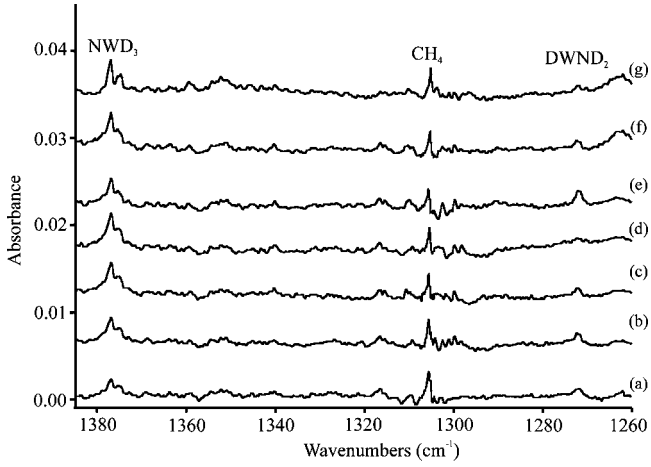

Figure 2. Infrared spectra for the tungsten atom reaction products with ND_3 in solid argon at 8 K: (a) deposition for 60 min; (b) after >530 nm irradiation; (c) after >470 nm irradiation; (d) after >320 nm irradiation; (e) after 240−380 nm irradiation; (f) after >470 nm irradiation; (g) after annealing to 25 K.

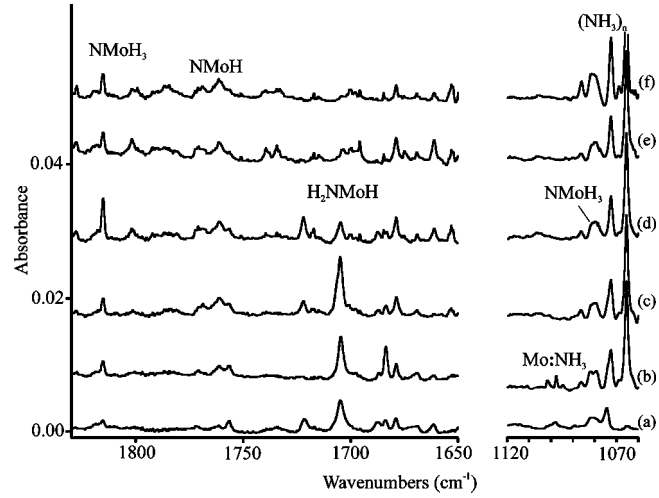

Figure 3. Infrared spectra for the molybdenum atom and NH_3 reaction products in solid argon at 8 K: (a) deposition for 60 min; (b) after annealing to 25 K; (c) after >530 nm irradiation; (d) after >320 nm irradiation; (e) after 240−380 nm irradiation; (f) after annealing to 30 K.

absorption at 1081 cm^{-1} on top of a broad feature exhibited the same photolysis behavior. Another band at 1704.1 cm^{-1} decreased on >320 nm irradiation and annealing to 25 K but increased on 240−380 nm irradiation, which seems to be at the expense of the 1815.4 cm^{-1} band. One band at 1761 cm^{-1} on deposition increased on near-UV irradiation. These bands did not yield isotopic shifts with the $^{15}NH_3$ sample, but with the ND_3 sample all Mo−H bands shifted into the Mo−D stretching region, as shown in Table 2.

Chromium. Several experiments were performed with chromium and ammonia. Unfortunately, the Cr−H stretching region is partially covered by the ammonia precursor absorption, but a new band at 1614.3 cm^{-1} increases on stepwise irradiation in concert with the decrease in new absorptions at 1100.2, 1095.9 cm^{-1}. The latter absorption increases on annealing then decreases 20% on >420 nm, 80% on >380 nm, and completely on >320 nm irradiation while the former band increases. Figure 4 illustrates an informative series of infrared spectra. Subsequent annealing replaces part of the 1100 cm^{-1} absorption but decreases the 1614.3 cm^{-1} band. An investigation with $^{15}NH_3$ gave the same 1614.3 cm^{-1} band and a shift of the lower band to 1095.0, 1090.4 cm^{-1}. With the deuteriated precursor, the product absorption at 1165.0 cm^{-1} reveals the same photochemistry as the 1614.3 cm^{-1} band, but it clears the ND_3 precursor absorption more than the hydrogen counterpart (see Figure 5).

Calculations. DFT calculations were done for the W−NH_3, Mo−NH_3, and Cr−NH_3 systems and the energy profiles and optimized geometries are illustrated in Figures 6 and 7. The

Table 2. Observed and Calculated Harmonic Frequencies of the N≡WH_3 and N≡MoH_3 Molecules in the Singlet Ground Electronic States with C_{3v} Structures[a]

	N≡WH_3					N≡MoH_3				
approx descripn	obsd	calcd (L)	intens	calcd (W)	intens	obsd	calcd (L)	intens	calcd (W)	intens
M−H str, a_1	1924	1992	48	1962	34		1926	44	1890	31
M−H str, e	1917	1984	392	1957	304	1815	1924	442	1893	336
M≡N str, a_1	1092	1142	56	1110	41	1081[c]	1154	68	1119	52
MH_2 bend, e	n.o.[b]	857	60	875	48		839	126	858	118
MH_3 def, a_1		691	39	666	32		686	42	640	48
NMH def, e		685	16	680	20		662	55	677	46

[a] Frequencies and intensities are in cm^{-1} and km/mol, respectively. All observed signals were in an argon matrix. Frequencies and intensities were computed with B3LYP (L) and BPW91 (W) methods in the harmonic approximation. Symmetry notations are for C_{3v}. [b] Not observed due to masking by broad absorption. [c] Weak band on side of broad absorption.

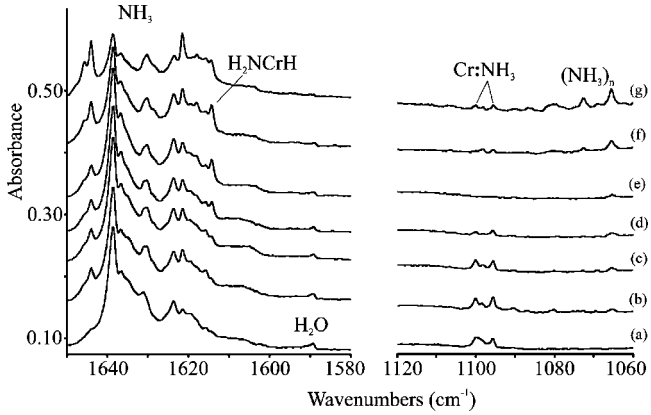

Figure 4. Infrared spectra for chromium atom and NH_3 reaction products in solid argon at 8 K: (a) deposition for 60 min; (b) after annealing to 20 K; (c) after >470 nm irradiation; (d) after >380 nm irradiation; (e) after 320 nm irradiation; (f) after annealing to 25 K; (g) after annealing to 30 K.

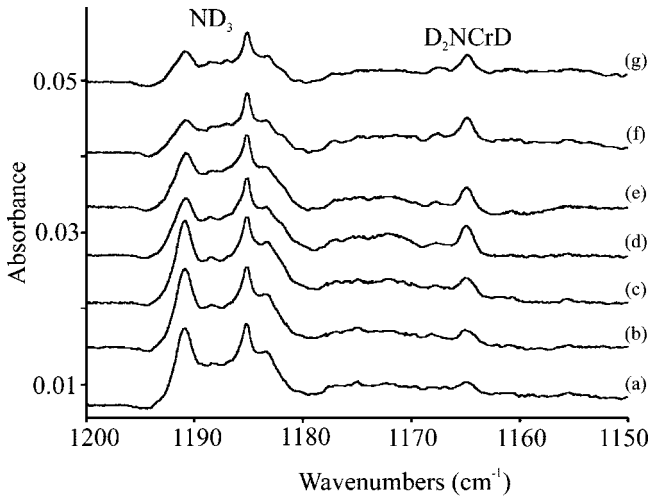

Figure 5. Infrared spectra for chromium atom reaction products with ND_3 in solid argon at 8 K: (a) deposition for 60 min; (b) after >470 nm irradiation; (c) after >380 nm irradiation; (d) after >290 nm irradiation; (e) after 240−380 nm irradiation; (f) after annealing to 20 K; (g) after annealing to 25 K.

NWH_3 molecule with C_{3v} symmetry was found to have the lowest energy, while the $HNWH_2$ and H_2NWH molecules are respectively 9 and 32 kcal/mol higher in energy. The tungsten ammonia complex W:NH_3, is calculated to have a $^5A_1$ ground state, which is located highest (52 kcal/mol above NWH_3) on the potential energy surface. The analogous $NMoH_3$ molecule with C_{3v} symmetry is the global minimum, $HNMoH_2$ is almost identical in energy (only 1 kcal/mol higher at this level of theory), and H_2NMoH is 3 kcal/mol higher. As expected, the molybdenum ammonia complex with a $^5A_1$ ground state lies highest in energy (20 kcal/mol). Similarly, the geometry parameters were calculated for the analogous chromium species, but the energy profile shows that H_2NCrH is the global minimum species (Figure 6).

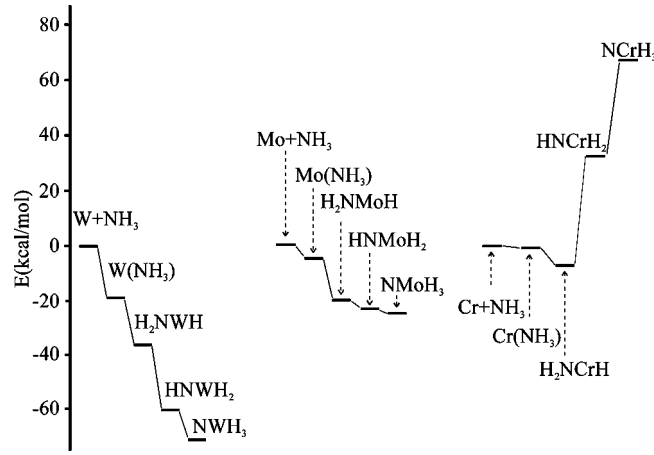

Figure 6. Energy profiles for isomers of M−NH_3 computed at the B3LYP level of theory.

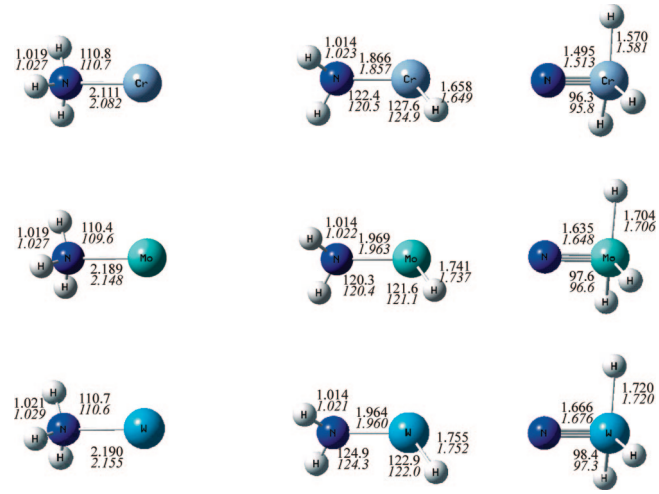

Figure 7. Optimized structures for products of the group 6 metal and ammonia reactions. Parameters are given for B3LYP and BPW91 (in italics). Bond lengths are in angstroms and angles in degrees.

Discussion

The new absorptions from products of group 6 metal atom oxidative addition reactions with NH_3 will be identified through

thermochemical and photochemical properties, isotopic substitution, and comparison with theoretical frequency calculations.

M:NH_3 Complex (M = W, Mo, Cr). A very weak band at 1188.0 cm^{-1} appeared in the laser-ablated W atom reaction with NH_3, increased markedly on annealing to 20 K, but totally disappeared on >470 nm irradiation, which increased the final product. With $^{15}NH_3$ this band shifted to 1181.8 cm^{-1}, but with ND_3 this band fell underneath the precursor, which is characteristic of the symmetric bending mode of NH_3 perturbed by a metal atom. The mixed $^{14}NH_3 + {}^{15}NH_3$ experiment gave two bands at 1188.0 and 1181.8 cm^{-1}. This shift, 5.2%, is characteristic of the ammonia symmetric deformation mode. Therefore, the 1188.0 cm^{-1} band is assigned to the W:NH_3 complex (1:1), which is the first step in the activation of ammonia by metal atoms. Note that similar bands in solid argon were observed for Th:NH_3 at 1149.8 cm^{-1}, Zr:NH_3 at 1156.0 cm^{-1}, and Hf:NH_3 at 1158.8 cm^{-1}.[7,8]

A similar photosensitive band at 1100.8 cm^{-1} (site 1097.6 cm^{-1}) was observed in laser-ablated Mo atom reactions with NH_3, which appeared weakly on deposition, increased markedly on annealing to 20 and 25 K, but disappeared on >530 nm irradiation. The ^{15}N-substituted band shifts to 1094.9 cm^{-1} (site 1091.7 cm^{-1}), a 5.3% shift. The analogous Mo:NH_3 complex was identified. A similar pair of matrix-split bands at 1100.2, 1095.9 cm^{-1} is assigned as Cr:NH_3.

Our B3LYP functional calculations support these assignments. The W:NH_3 complex was calculated to have a $^5A_1$ ground state with a strong symmetric N−H deformation mode at 1220 cm^{-1}, which is 193 cm^{-1} above that calculated for ammonia itself. The complex is observed 213 cm^{-1} blue-shifted from ammonia in solid argon, which is in very good agreement with experiment. Likewise, the Mo:NH_3 complex was predicted at 1180 cm^{-1}, which is 153 cm^{-1} above the ammonia calculation, and the complex at 1101 cm^{-1} is 126 cm^{-1} above the argon matrix ammonia band. In like fashion, the Cr:NH_3 complex was calculated with a $^5A_1$ ground state and a strong symmetric N−H deformation mode at 1174 cm^{-1}, which is 149 cm^{-1} above that calculated for ammonia itself, whereas the observed 1096 cm^{-1} band is 121 cm^{-1} above the precursor band in solid argon.

N≡MH_3 (M = W, Mo). The very high frequency absorption observed at 1917.0 cm^{-1} on deposition of laser-ablated W atoms with NH_3 tracks with a weak band at 1924.1 cm^{-1} in the W−H stretching region and a weak band at 1092.2 cm^{-1} in the W−N stretching region.[17,32] These bands increased twofold on >470 nm irradiation and decreased on 240−380 nm irradiation, which caused an increase of another product absorption at 1771.5 cm^{-1} (Figure 1). In another experiment this group of absorptions doubled in intensity on >530 and >380 nm irradiation, decreased on 240−380 nm irradiation, and increased again with >530 nm irradiation. The two W−H stretching absorptions are slightly lower than this mode for WH_6 in argon but higher than for the remaining tungsten hydrides.[17] With ND_3 the two upper bands shift into one band, 1377.0 cm^{-1}, which defines the 1.392 H/D ratio that is expected for tungsten hydrides. The W−N stretching frequency is 33 cm^{-1} higher than the diatomic W≡N molecule fundamental in solid argon,[32] suggesting triple-bond character. With $^{15}NH_3$ the two upper W−H stretching modes show no shift, but the W−N stretching mode shifts to 1058.4 cm^{-1} (3.09%), which is similar to that for the W≡N diatomic molecule. This group of bands can be assigned to W−H and W−N stretching modes of the N≡WH_3 molecule. It interesting that the N≡WF_3 molecule exhibits almost the same W≡N stretching fundamental: namely, 1091.1 cm^{-1}.[21]

The strongest absorption of N≡MoH_3 was observed in laser-ablated Mo atom reactions with NH_3 in solid argon. A weak band at 1815.4 cm^{-1} in the Mo−H stretching region appeared on deposition, increased twofold on annealing to 20 K and sixfold on >320 nm irradiation, but decreased on 240−380 nm irradiation. With $^{15}NH_3$ this band shows no shift. With ND_3 the counterpart Mo−D stretching frequency should be around 1305 cm^{-1}, where it would be covered by a CH_4 impurity (from cracking of silicone diffusion pump oil) band at 1305 cm^{-1} in solid argon. A weak 1081 cm^{-1} peak is associated on photolysis, but the ^{15}N and D isotopic counterparts were not found with $^{15}NH_3$ and ND_3 because of overlap with precursor bands. This band is broadened by molybdenum isotopic dilution, but recall that molybdenum isotopic splitting was resolved for the counterpart absorption at 1075 cm^{-1} for the analogous N≡MoF_3 molecule.[21] Following this reasoning, the 1081 cm^{-1} peak probably corresponds to the most abundant ^{98}Mo counterpart.

The assignments to N≡WH_3 and N≡MoH_3 are confirmed by B3LYP harmonic frequency calculations. For the N≡WH_3 molecule the calculation predicted a strong degenerate W−H antisymmetric mode at 1983.9 cm^{-1}, a weak W−H symmetric mode at 1992.5 cm^{-1}, and a weak W−N stretching mode at 1142.3 cm^{-1}, which are in very good agreement with experimental values (overestimated by 3.5%, 3.6%, and 6.1%). The observed 7.1 cm^{-1} symmetric−antisymmetric W−H stretching mode separation is matched by the calculated 7.6 cm^{-1} separation. The W≡N stretching mode is predicted to shift 3.11% on ^{15}N substitution, which is in excellent agreement with the observed 3.09% shift. In the N≡WD_3 case, this mode separation is predicted to be 0.2 cm^{-1}, and we observed only one band, at 1377.0 cm^{-1}. Calculation for N≡MoH_3 gave a strong degenerate Mo−H antisymmetric mode at 1921.8 cm^{-1} and a weak Mo−H symmetric mode at 1923.9 cm^{-1}, and we observe only a single band at 1815.4 cm^{-1} (overestimated by 5.4%).

Frequencies calculated with the BPW91 functional are slightly lower (Table 2), and they correlate well with the B3LYP values, which substantiates the application of density functional theory to support vibrational assignments for these molecules.[33,34]

H_2N−MH. The sharp band observed to split at 1772.2, 1770.9 cm^{-1} on deposition of W + NH_3 in solid argon decreased slightly on annealing to 20 K and depleted totally on >470 nm irradiation. However, this band was recovered on 240−380 nm irradiation. With ND_3 this band shifted to 1272.3, 1271.6 cm^{-1}, defining a 1.393 H/D ratio, which is appropriate for the W−H stretching vibration of the first insertion product H_2NWH. This is by far the strongest absorption calculated for this molecule. Unfortunately the W−N and NH_2 stretching modes due to this molecule are not observed because of band weakness.

The analogous Mo−H stretching mode of H_2NMoH was observed at 1704.5 cm^{-1} and decreased on >320 nm and 240−380 nm irradiation. With ND_3 the counterpart band was found at 1232.7 cm^{-1}, giving a 1.383 H/D ratio, which is essentially the same as the ratio found in molybdenum hydrides. Again, the strongest band calculated for this species is the Mo−H stretching mode at 1776 cm^{-1}.

The chromium photochemical product absorption at 1614.3 cm^{-1} shifts to 1165.0 cm^{-1} on deuterium substitution (H/D ratio 1.386), which is reasonable for a Cr−H stretching mode.[17] The

(32) Andrews, L.; Souter, P. F.; Bare, W. D.; Liang, B. *J. Phys. Chem. A* **1999**, *103*, 4649 (W + N_2).

(33) Scott, A. P.; Radom, L. *J. Phys. Chem.* **1996**, *100*, 16502.

(34) Andersson, M. P.; Uvdal, P. L. *J. Phys. Chem. A* **2005**, *109*, 3937.

Table 3. Observed and Calculated Vibrational Frequencies of the Group 6 H_2N-MH Insertion Product Molecules in the $^5A'$ Ground Electronic States with C_s Structures[a]

	H_2N-CrH					H_2N-MoH					H_2N-WH				
approx descripn	obsd[b]	calcd (L)	intens	calcd (W)	intens	obsd[b]	calcd (L)	intens	calcd (W)	intens	obsd[b]	calcd (L)	intens	calcd (W)	intens
N−H str		3577	13	3485	12		3568	21	3481	19		3567	23	3487	19
N−H str		3496	15	3400	11		3483	21	3400	15		3484	19	3403	11
M−H str	1614	1710	267	1702	225	1704	1776	283	1769	232	1772	1847	232	1837	205
NH_2 bend		1542	17	1493	12		1536	10	1486	7		1548	17	1498	13
M−N str		650	122	645	91		637	106	636	80		655	87	652	67
NH_2 rock		551	26	557	18		611	17	606	14		632	16	626	13
NH_2 def		551	110	547	91		509	105	490	108		494	140	479	141
M−H def		382	382	382	144		437	88	432	63		447	23	440	12
torsion		362	97	356	77		332	51	323	41		373	22	360	19

[a] Frequencies and intensities are in cm^{-1} and km/mol, respectively. Frequencies and intensities were computed with B3LYP (L) and BPW91 (W) methods in the harmonic approximation. [b] Observed in an argon matrix.

Table 4. Natural Orbital Occupation Numbers for $E{\equiv}MH_3$ Molecules and the Resulting Effective Bond Order (EBO)[a]

molecule	σ	π	σ^*	π^*	EBO
$N{\equiv}CrH_3$ (L)	1.94	3.89	0.09	0.10	2.82
$N{\equiv}MoH_3$ (C)	1.96	3.93	0.08	0.06	2.88
$N{\equiv}MoH_3$ (L)	1.96	3.96	0.08	0.04	2.90
$N{\equiv}MoH_3$ (W)	1.96	3.97	0.08	0.03	2.91
$N{\equiv}WH_3$ (C)	1.98	3.93	0.06	0.06	2.89
$N{\equiv}WH_3$ (L)	1.97	3.96	0.06	0.04	2.92
$N{\equiv}WH_3$ (W)	1.98	3.97	0.06	0.03	2.93
$HC{\equiv}MoH_3$ (L)	1.96	3.94	0.07	0.04	2.89
$HC{\equiv}MoH_3$ (W)	1.96	3.97	0.07	0.04	2.90
$HC{\equiv}WH_3$ (L)	1.98	3.97	0.05	0.04	2.91
$HC{\equiv}WH_3$ (W)	1.98	3.95	0.05	0.04	2.92

[a] Values for π orbitals summed over both components; (C) denotes the CCSD method, (L) the B3LYP functional, and (W) the BPW91 functional.

first insertion product, H_2NMoH, is the most stable species in this system, and the strong Cr−H stretching mode is calculated as 1710 cm^{-1} (Table 3), which is 5.9% higher than the observed value and is in accord with the other first insertion products.

Our B3LYP calculations predicted the W−H stretching mode of H_2NWH molecule at 1847 cm^{-1}, an overestimate of 4.2%, which is the expected agreement with the experimental value.[20] Recall the calculated W−H stretching modes of tungsten hydrides are 3−4% higher than observed values.[17] The calculated Mo−H stretching frequency of H_2NMoH at 1776 cm^{-1} is 4.1% high and correlates with experiment very well. The trend in calculated and observed M-H stretching frequencies for these three insertion products (Table 3) shows that density functional theory is a very good approximation for these molecules.

NMoH. A weak band at 1761 cm^{-1} doubled in intensity on >530 nm irradiation and remained constant throughout the rest of the experiment. This band is 54 cm^{-1} below the strong Mo−H stretching mode of the $N{\equiv}MoH_3$ molecule, and our calculation predicts the strong Mo−H stretching modes of NMoH to fall 104 cm^{-1} lower. This band shows no ^{15}N shift, but it was too weak to observe on deuterium substitution. We have insufficient information to identify NMoH conclusively, but this possibility should be considered.

Reaction Mechanisms. Combination of chromium, molybdenum, or tungsten atoms with NH_3 gives the straightforward intermediate $M{:}NH_3$ complex trapped in the cold argon matrix.

$$M + NH_3 \rightarrow M{:}NH_3 \quad (1)$$

Reaction 1 is exothermic by 7, 7, and 20 kcal/mol for Cr, Mo and W, respectively. The more exothermic value for W can be reasoned by the notion that the lower W atom ground state holds the electron pair from NH_3 with less repulsion. This intermediate complex rearranges exothermically to the insertion product H_2N-MH for all three metals (see Figure 6), and further rearrangement through $HN{=}MH_2$ to $N{\equiv}MH_3$ is exothermic for Mo and W only (reaction 2).

$$M{:}NH_3 \rightarrow H_2N-MH \quad (2)$$

Upon >530 nm irradiation the H_2N-MH intermediate photochemically isomerizes to $N{\equiv}MH_3$, but with 380−240 nm irradiation, the rearrangement reverses (reaction 3).

$$H_2N-MH \leftrightarrow N{\equiv}NH_3 \quad (3)$$

Remember that annealing increases the $N{\equiv}WH_3$, H_2N-MoH, $N{\equiv}MoH_3$, and H_2N-CrH products: this means that the reaction of naked group 6 metal atoms with ammonia is spontaneous. A similar conclusion was reached for thorium, as $HN{=}ThH_2$ was formed on annealing.[15] Here, however, we do not trap the $HN{=}MoH_2$ and $HN{=}WH_2$ intermediates as the reaction goes on to the more stable final products.

$$M + NH_3 \rightarrow M{:}NH_3 \rightarrow H_2N-MH \rightarrow N{\equiv}MH_3 \quad (4)$$

In the laser-ablation process the $N{\equiv}MH_3$ molecule can be photodecomposed to give $N{\equiv}MH$. Reaction 5 is endothermic by 115 and 20 kcal/mol for W and Mo, respectively, which may account for the possible observation of the Mo and not the W species.

$$N{\equiv}MH_3 + \text{photons} \rightarrow N{\equiv}MH + H_2 \quad (5)$$

Bonding. Since the d electrons of tungsten and molybdenum are strongly involved in σ bonding, reactions of Mo and W with NH_3 gave major stable high-oxidation-state products, $N{\equiv}MoH_3$ and $N{\equiv}WH_3$, which are in agreement with the DFT calculated energy profile (Figure 6). By the same rationale tungsten (molybdenum) hexahydride, WH_6, has been identified in the W atom reaction with H_2 in a low-temperature matrix.[17] Tungsten atom reactions with H_2O_2, giving tungsten hydride oxide, H_2WO_2, is another example of d orbital participation in σ bonding.[16]

Natural orbital occupations have been calculated for the $N{\equiv}MoH_3$ and $N{\equiv}WH_3$ molecules using the CCSD wave function based method[23] and two density functionals, and the results are given in Table 4. These occupations are approximate, as 6.03 electrons occupy this six orbital set instead of the expected 6.00. The effective bond order is total bonding minus total antibonding divided by 2. We see that the EBO for the W≡N triple bond is 2.89, 2.92, or 2.93 and for the Mo≡N triple bond is 2.88, 2.91, or 2.90, depending on the theoretical method employed. These are fully developed triple bonds, and the EBO's are essentially the same for $HC{\equiv}MoH_3$ and $HC{\equiv}WH_3$, computed in the same manner. A slight increase in EBO for

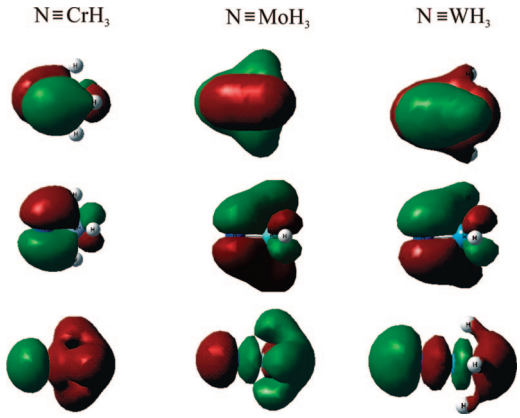

Figure 8. HOMO's for triple bonds in the $N{\equiv}CrH_3$, $N{\equiv}MoH_3$, and $N{\equiv}WH_3$ molecules calculated with B3LYP/SDD/6-311++G(3df,3pd). The isodensity level is 0.03 e/au^3.

the heavier metal species was also observed for the analogous $N{\equiv}MoF_3$ and $N{\equiv}WF_3$ molecules.[21]

The bonding molecular orbitals for $N{\equiv}CrH_3$, $N{\equiv}MoH_3$, and $N{\equiv}WH_3$ are plotted in Figure 8. We see mixing of the M−H and M−N bonding orbitals in varying degrees. Finally, the EBO for $N{\equiv}CrH_3$ using the B3LYP method is 2.82, but this molecule is not formed, owing to weakness of the Cr−H bonds relative to the N−H bonds in the ammonia precursor.

The bonding and structure of the $N{\equiv}MoH_3$ and $N{\equiv}WH_3$ molecules have been considered theoretically by Firman and Landis,[10] and our computed DFT structures are in agreement. As discussed by these authors, the two π bonds in $N{\equiv}WH_3$ form a cylinder of electron density around the W−N bond, and maximization of the π bonding locates the W−H bonds in the plane perpendicular to the W−N bond.

It is interesting to compare the structures of $N{\equiv}WH_3$ and $N{\equiv}WF_3$ (Figure S1 in the Supporting Information). First, the H−W−H angle in $N{\equiv}WH_3$ is 4.5° larger than the F−W−F angle in $N{\equiv}WF_3$. Second, the W≡N triple bond is highly polarized in $N{\equiv}WF_3$ because of fluorine electronegativity, although the W≡N bond lengths are essentially the same for both molecules. These molecular structures clearly violate the traditional VSEPR model, since stronger F−F atom repulsion in $N{\equiv}WF_3$ yields a smaller F−W−F angle than weaker H−H atom repulsion in $N{\equiv}WH_3$ yields a larger H−W−H angle. The π bonding between ligand and metal center and ligand−ligand repulsion must play critical roles in the bonding.[35] For $N{\equiv}WF_3$ the p electron pair from the F atom donates to d orbitals on the W center to form a π bond, which leads to the regular VSEPR structure. However, the F−F ligand repulsion makes the F−W−F angle larger than 90°. For $N{\equiv}WH_3$ the H atom does not have p electrons and only H−H repulsion leads to a larger H−W−H bond angle. Similar F−W−F bond angles in $N{\equiv}WF_3$ and $P{\equiv}WF_3$ suggest that polarization of the outmost core shell of the tungsten center is not very important. Note that for main-group-metal hydrides the core polarization favors bent structures of BaH_2 and SrH_2.[36]

Many tungsten and molybdenum complexes have been found to violate the traditional VSEPR bonding model. For example valence-bonded WH_6 and MoH_6 have been confirmed both experimentally and theoretically as trigonal-prismatic C_{3v} structures.[17,37] The analogues $W(CH_3)_6$ and $Mo(CH_3)_6$ have been characterized by a C_{3v} skeleton.[38] However, tungsten and molybdenum hexahalides favor O_h structures because of strong ligand−ligand repulsion and available π bonding, as shown in Figure S2 (Supporting Information).

The terminal Mo≡N and W≡N triple bonds investigated here have computed bond lengths (Figure 7) which are in agreement within the error of calculation with measurements made on larger organometallic $L_3Mo{\equiv}N$ and $L_3W{\equiv}N$ complexes, 1.634 and 1.669 Å, respectively.[18,19] In addition, the computed triple-bond lengths for our $H_3Mo{\equiv}N$ and $H_3W{\equiv}N$ complexes are essentially the same as calculated by the B3LYP density functional and at the higher CASSCF/CASPT2 level of theory for the analogous $F_3Mo{\equiv}N$ and $F_3W{\equiv}N$ complexes[21] and are about 2% shorter than bond lengths taken from tabulated triple-bond radii.[39] Hence, the B3LYP density functional does a very good job of describing the terminal Mo≡N and W≡N triple bonds investigated here.

It is also interesting to compare the product energy profile for methane reactions[20] with the products from ammonia. With chromium, the insertion product is the global minimum energy species for both reactions. With molybdenum, all products are closer in energy but the insertion product is lowest for methane and highest for ammonia. With tungsten, the strength of the W−H bond contributes to promote maximum hydrogen transfer and make the triple-bonded species the global minimum for both precursors.

Conclusions

Reactions of laser-ablated chromium, molybdenum, and tungsten atoms with ammonia during condensation in excess argon give the $H_2N{-}MH$ insertion product, which rearranges to $N{\equiv}MoH_3$ and $N{\equiv}WH_3$, but $N{\equiv}CrH_3$ is too high in energy to be formed here. The subject molecules were trapped in solid argon and identified by isotopic shifts and DFT frequency calculations. The 1:1 metal−ammonia complexes were formed on annealing and photoisomerized to the above products. Annealing increases the sharp product absorptions, which indicates a spontaneous reaction between group 6 metal atoms and ammonia molecules. The $N{\equiv}MoH_3$ and $N{\equiv}WH_3$ molecules contain fully developed triple bonds with effective bond orders near 2.9, computed using CCSD and density functional methods. Furthermore, the triple-bond lengths calculated here for the simple $N{\equiv}MoH_3$ and $N{\equiv}WH_3$ molecules are in agreement with experimental measurements for larger $N{\equiv}MoR_3$ and $N{\equiv}WR_3$ organometallic complexes.[18,19]

Acknowledgment. We gratefully acknowledge financial support from NSF Grant No. CHE 03-52487 and NCSA computing Grant No. CHE07-0004N to L.A.

Supporting Information Available: Figures S1 and S2, comparing structures with H and F substituents. This material is available free of charge via the Internet at http://pubs.acs.org.

OM8003459

(35) (a) Kaupp, M. *Angew. Chem., Int. Ed.* **2001**, *40*, 3534. (b) Straka, M.; Hrobarik, P.; Kaupp, M. *J. Am. Chem. Soc.* **2005**, *127*, 2591.

(36) Wang, X.; Andrews, L. *J. Phys. Chem. A* **2004**, *108*, 11500.

(37) (a) Shen, M.; Schaefer, H. F., III; Partridge, H. *J. Chem. Phys.* **1993**, *98*, 508. (b) Kang, S. K.; Tang, H.; Albright, T. A. *J. Am. Chem. Soc.* **1993**, *115*, 1971. (c) Tanpipat, N.; Baker, J. *J. Phys. Chem.* **1996**, *100*, 19818. (d) Kaupp, M. *J. Am. Chem. Soc.* **1996**, *118*, 3018. Shen, M.; Schaefer, H. F., III; Partridge, H. *J. Chem. Phys.* **1993**, *98*, 508 (WH_6 theoretical calculations).

(38) (a) Pfennig, V.; Seppelt, K. *Science* **1996**, *271*, 626. (b) Hleinhenz, S.; Pfennig, V.; Seppelt, K. *Chem. Eur. J.* **1998**, *4*, 1687. (c) Haaland, A.; Hammel, A.; Rypdal, K.; Volden, H. V. *J. Am. Chem. Soc.* **1990**, *112*, 454.

(39) Pyykko, P.; Riedel, S.; Patzschke, M. *Chem. Eur. J.* **2005**, *12*, 3511.